A Novel Linear Direct Drive System for Textile Winding Applications

Nigel JAKEMAN, William BULLOUGH, Chris BINGHAM
Faculty of Engineering, University of Sheffield
Mappin Street
Sheffield, UK, S1 3JD
Tel: 00 44 (0)114 2225195, Fax: 00 44 (0)114 2225196
E-mail: nigel.jakeman@newage-avkseg.com, (w.bullough,c.bingham)@sheffield.ac.uk

Prof. Phillip MELLOR
Department of Electrical & Electronic Engineering, University of Bristol
Woodland Road, Clifton
Bristol, UK, BS8 1UB
Tel: 00 44 (0)117 9545168 , Fax: 00 44 (0)117 9545206
e-mail: p.h.mellor@bristol.ac.uk

Acknowledgements

The authors wish to express their sincerest thanks to the EPSRC (UK) for funding the research.

Keywords

<< Linear drives >> << Motion control >> << Permanent magnet motors >> << Brushless drives >> << Actuators >>

Abstract The paper describes the specification, modelling, magnetic design, thermal characteristics and control of a novel, high acceleration (up to 82g) brushless PM linear actuator with Halbach array, for textile package winding applications. Experimental results demonstrate the realisation of the actuator and induced performance advantages afforded to the phase lead, closed-loop position control scheme.

1 Introduction

Industry is always looking to develop new processes and machinery so that the quality of its output can be improved and operational costs reduced. To facilitate this, two key areas of design are pertinent viz. speed of operation, and the flexibility of control of manufacturing machinery. Reconfiguration of current manufacturing machinery often involves the replacement of linkage mechanisms forming the mechanical advantage and velocity magnifier. Under highly demanding operating conditions, the materials from which these mechanisms are made experience excessive stresses, and unpredictable manufactured fatigue limits are often exceeded.

Here then, a new genre of machine is investigated to address the speed of response of a system to a change in operational requirements, whilst still offering an adequate supply of force, velocity and displacement [1] required to achieve demanding dynamic profiling applications. The system realised herein to demonstrate the theory ultimately achieves the inherent properties required to meet the performance levels desired, whilst attaining the level of electronic reconfiguration demanded by modern day manufacturing.

2 Linear Actuator Specification

The proposed actuator concept is applied to a highly demanding textile winding application, fig.1. During turnaround periods at either end of the traverse, the actuator must be capable of accelerations in the region 50-100g, and the winding velocity equal to 5 m/s over the stroke length of 250mm. Although, in theory, electro-rheological fluid clutches could satisfy the acceleration requirements, to-date, the fluid specification to realise such performance has yet to be achieved [2]. An alternative solution has therefore been realised using a direct drive linear actuator.

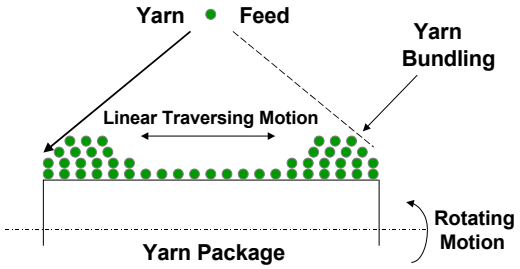

Fig.1: Yarn bundling in the textile industry.

2.1 Magnetic design

A brushless tubular PM linear actuator with Halbach array, fig 2(a), has been realised to address the demonstrator specification. The self-shielding nature of the Halbach array [3], see fig.2(b), yields a demonstrator design with low output mass and ironless stator; thus ensuring a topology with low electrical and mechanical time constants. Furthermore, the elimination of soft magnetic material permits the use of effective water cooling to increase the electrical loading of the machine itself. The radial component of magnetic flux density in the airgap, B_r, is acquired in the usual manner by considering a magnetic boundary model with equivalent current sheets and solving for the vector magnetic potential using the separation of variables technique:

$$B_r = \frac{\mu_0 H_c}{2}\left[e^{\lambda(r-2r_2+r_1)} - e^{\lambda(r-r_1)}\right]\cos(\lambda z) \tag{1}$$

where H_c is the coercivity of the permanent magnets and λ is the spatial wave number of the array, equal to $2\pi / l_p$; r_1 and r_2 are the internal and external radii of the magnet array, respectively. Integrating the flux density for the for the winding region and dividing by its depth, r_o-r_i, yields the true average flux density, B_{ave}, from which the current density, J, required for a given axial thrust, F_z, can be computed from the commutation relationship:

$$\begin{bmatrix} J_a \\ J_b \end{bmatrix} = \left(\frac{F_z}{\sqrt{2} B_{ave} (r_o - r_i)(r_i + r_o) l_p k_p p_m} \right) \begin{bmatrix} \cos(\lambda z) \\ \sin(\lambda z) \end{bmatrix} \tag{2}$$

where k_p, l_p and p_m are the winding packing factor, pole pair pitch and number of pole pairs in the magnet array, respectively.

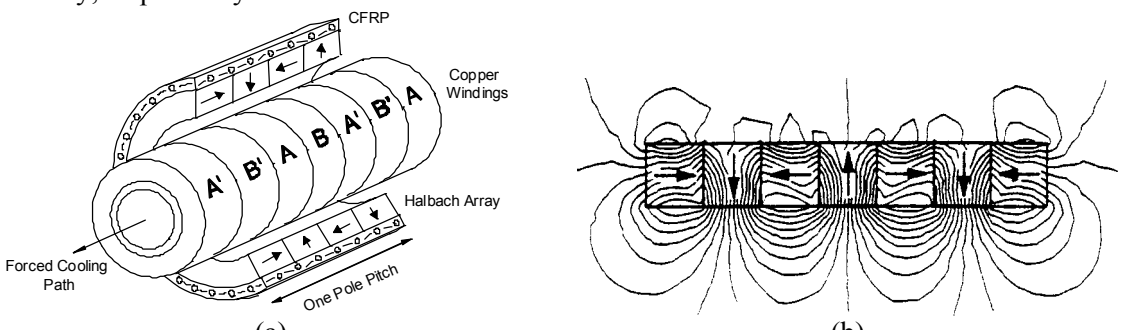

(a) (b)

Fig.2: (a) 2-phase linear actuator with Halbach array (b) Self shielding Halbach array

2.2 Thermal design

The stator windings, of electrical conductivity $\sigma\left(\Omega^{-1}m^{-1}\right)$, are wound onto a simple tube, known as the former, of internal radius r_f, mean radius, r_m, thickness x_f and of material with thermal conductivity k ($Wm^{-1}K^{-1}$). Water, of temperature T_c at the inlet, is passed through the tube at a known flow rate, from which the Prandtl, Reynolds and Nusselt numbers for the tube can be calculated [4] to yield a heat transfer coefficient, h ($Wm^{-2}K^{-1}$), which ultimately determines the surface temperature of the windings T_w:

$$T_w = \frac{J^2}{2\sigma k_p}(r_0^2 - r_i^2)\left(\frac{x_f}{kr_m} + \frac{1}{hr_f}\right) + T_c \qquad (3)$$

2.3 Demonstrator machine design

A design approach was undertaken to optimise the actuator for minimal winding temperature rise for a given velocity profile demand. However, the optimised actuator was not practical to build within the financial constraints imposed on the project, and a demonstrator machine was therefore constructed primarily for the purpose of model validation. The actuator geometry yielded a moving component with a mass of 13 grams and a two phase stator with 42 poles of 7mm pitch. An approximation of the idealised Halbach array was achieved using a two block per pole array with alternate axial and radial magnetised NdFeB pole pieces [5]. Electromagnetic finite element analysis, fig 3(a) confirmed a peak fundamental airgap flux density 0.406 T, and verified the force constant of 0.42 N/A predicted using the analytical approach highlighted above. Thermal FEA, fig 3(b), and practical validation confirmed a maximum winding temperature of 153°C for the desired 120 A/mm^2 RMS winding current density.

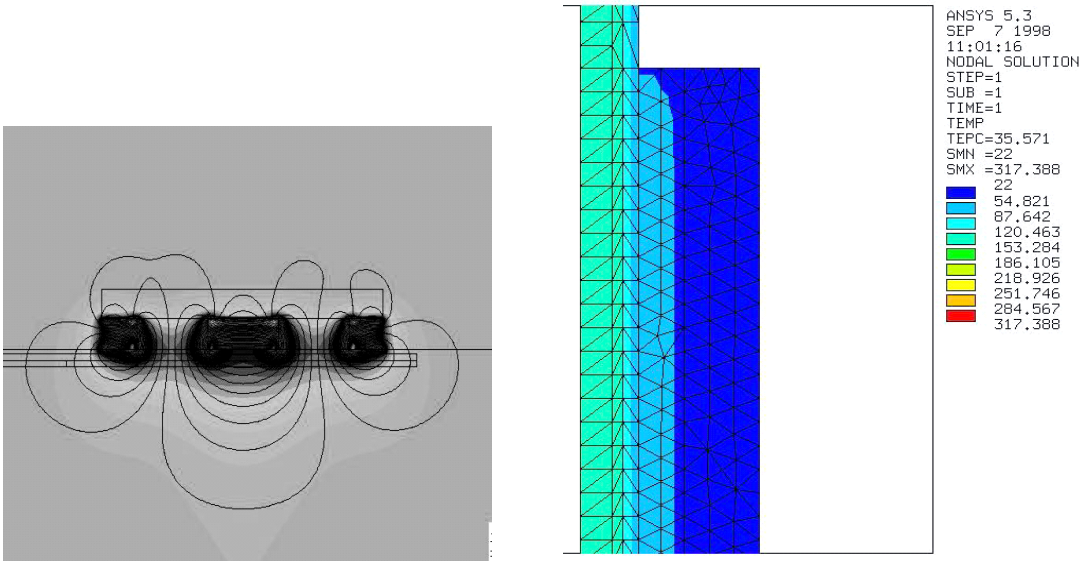

(a) (b)

Fig.3: (a) Electromagnetic and (b) Thermal FEA

3 Actuator Construction

Figure 4 shows the fully assembled demonstrator actuator. Hall-effect position sensors are located across the full axial length of the stator to determine the position of the array from permanent magnets located on the underside of the moving element. To provide structural integrity, both the magnet array and the stator windings were impregnated in a Kevlar fibre reinforced composite matrix. Bearing of the moving output is achieved using PTFE axial-orientated strips in contact with the surface of the stator itself.

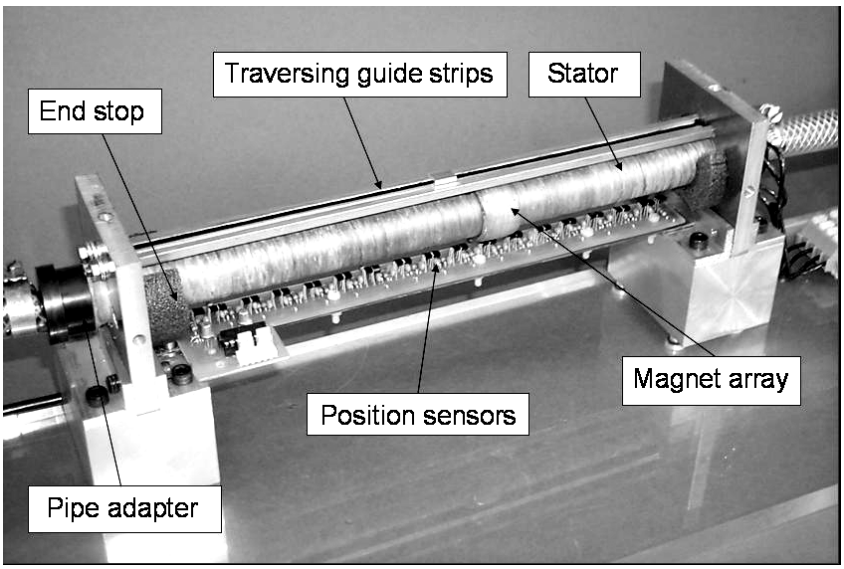

Fig.4: Prototype linear actuator

4 System Overview

Both phases of the actuator are controlled independently using separate four quadrant, Pulse Width Modulated electrical drives. An analogue, unipolar current controller with PI tuning modulates the gate drive signals to provide closed loop current control. Information from the Hall effect position sensors is decoded in the Digital Signal Processor (DSP) to provide the correct commutation switching sequence and to interpret the position of the actuator output. A phase lead position controller is implemented in the DSP to yield the correct position demand from the error and demand signals. The real time simulation used to model the system is illustrated in fig. 5.

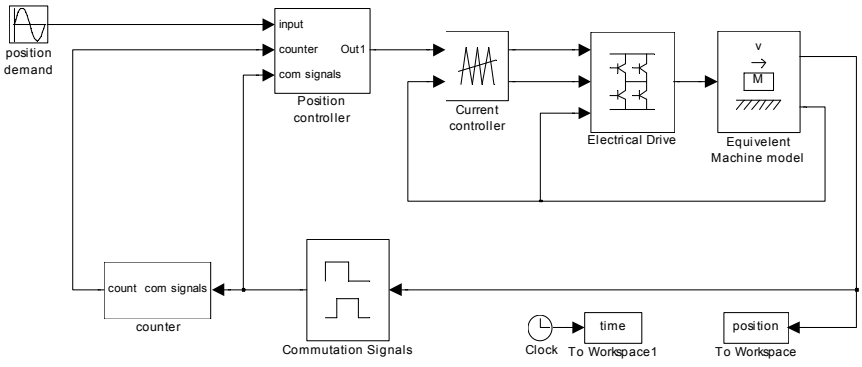

Fig.5: Real time simulation system model

5 Controller Development

The uncompensated second order system exhibits a classically under-damped characteristic with a damping ratio of $\zeta \approx 0.1$ and undamped natural frequency of 6.6 Hz. A closed loop position control system was modelled with phase lead compensation to damp the response and improve the system bandwidth. Designed using frequency domain analysis, a transfer function for the compensation network was derived in continuous time as:

$$G_c(s) = 0.023\frac{(0.088s+1)}{(0.0022s+1)} \tag{4}$$

The Tustin transformation is applied to the controller transfer function to derive a compensation network in discrete time:

$$G_c(z) = 0.023\frac{(0.1761z-0.1759)}{(0.0045z-0.0043)} \tag{5}$$

Figure 6 illustrates the position controller model used to simulate the system performance with the discrete compensation network (5).

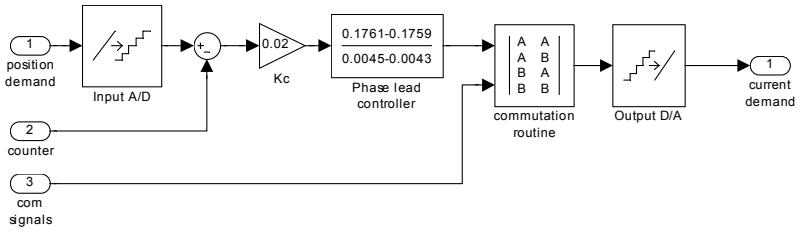

Fig.6: Position controller sub-system

6 Demonstrator System Performance

6.1 Steady state performance

The demonstrator system was tested with the discrete-time phase lead position controller. Figure 7 shows the frequency response characteristic, from which, a more critically damped system is evident. A full stroke (180mm) position control bandwidth of 7.5 Hz was observed, illustrating good correlation with that predicted using the simulation model presented in fig. 5.

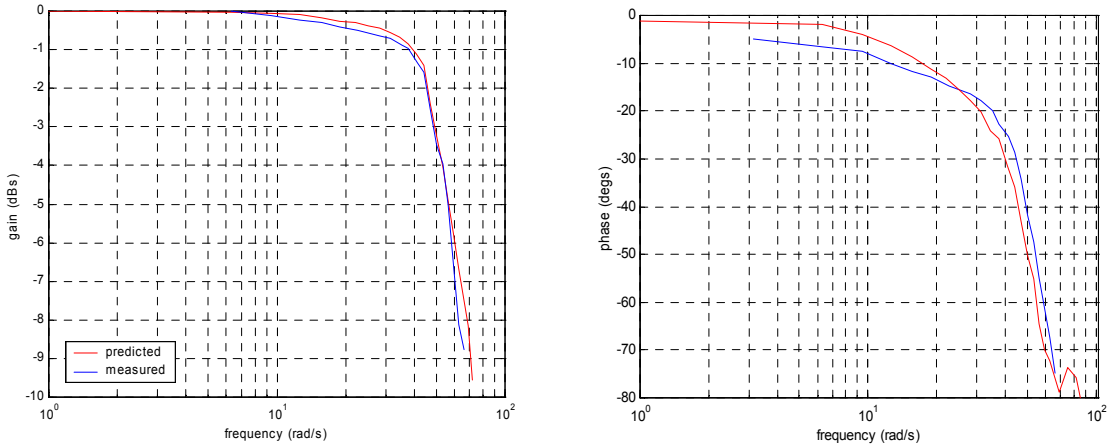

(a) (b)

Fig.7: Demonstrator system (a) gain and (b) phase response characteristic for full stroke operation

The true bandwidth of the system is projected to be 9.5 Hz. However, this performance was not realised practically due to the insufficient current delivery from the electrical drive. This constraint is reflected in the simulated and measured characteristics of fig. 7.

6.2 Transient performance validation

The transient response of the system to a step change in position demand is illustrated in fig. 8. Good correlation was achieved, and the transient response again reflects system operating without drive current saturation.

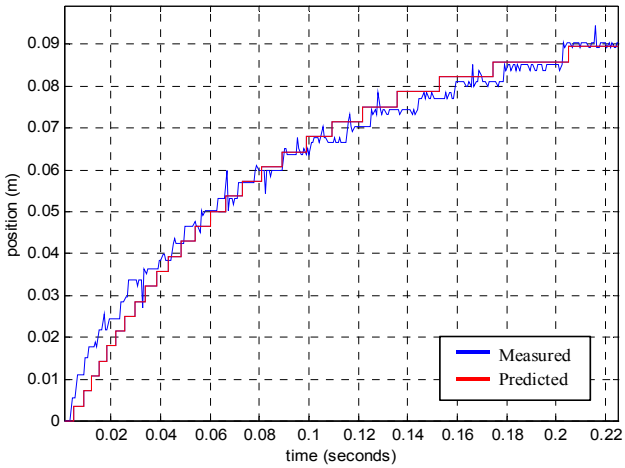

Fig.8: Demonstrator system transient response

7 Optimised System Performance

7.1 Optimised actuator design

Having verified the analytical, FEA and simulation models used to predict the performance of the system, an optimised actuator design was considered, neglecting the constraints discussed earlier. The actuator is considered to have an idealised Halbach array with 10.5 mm pole pair pitch, 0.57mm magnet length and 1.4mm stator depth. The resulting moving component has a mass of 6 grams and a corresponding force constant of 0.739 N/A.

7.2 Predicted performance

Illustrated in figure 9 is the full stroke (250mm) frequency response characteristic for the optimised system. An ultimate control bandwidth in excess of 220Hz is predicted for the system, however, the thermal limitation of the stator windings restricts this to a more modest 14.2 Hz; a value far in excess of the 9 Hz required for the textile winding system.

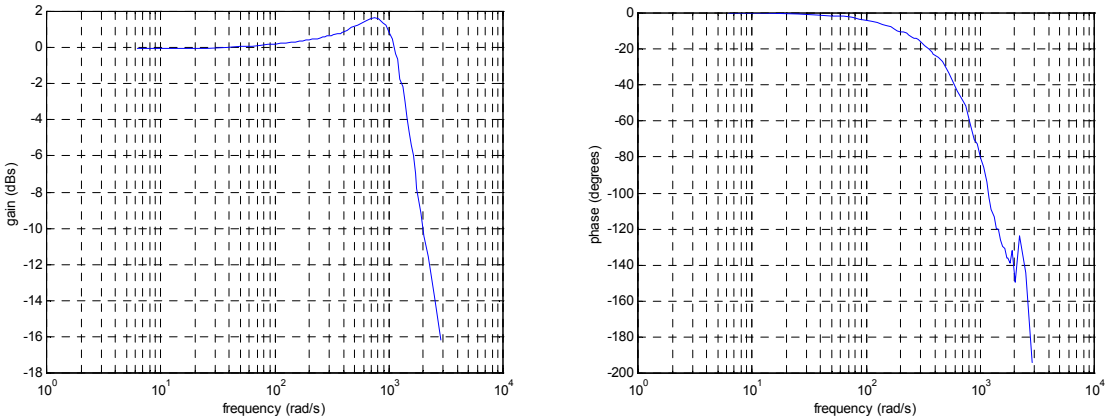

(a) (b)

Fig.9: Optimised system (a) gain and (b) phase response characteristic for full stroke operation

Figure 10 illustrates the ultimate performance that can be achieved for the textile winding demonstrator, taking into account the trapezoidal velocity profile required for the application. The corresponding acceleration of 82g for 5m/s linear traversing velocity is limited by the need to maintain a position accuracy of +/-0.25mm for the entire duration of the traversing cycle. This performance yields full speed turn round times of 12 ms at either end of the traverse, some 2 ms greater than the ultimate requirement of 10ms.

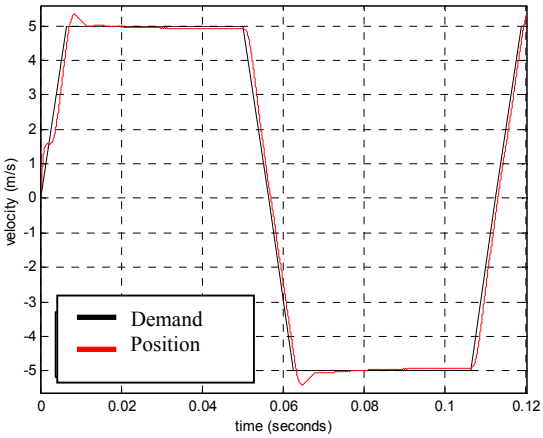

Fig.10: Ultimate textile winding performance

8 Conclusion

The specification, modelling and realisation of a novel linear actuator with Halbach array for a high-speed, high-acceleration textile winding application, have been described. Magnetic design, thermal modelling and dynamic control are addressed and verified using a practical demonstrator system. Re-evaluation of the system with an optimised actuator design yields performance projections of 82g linear acceleration and 14.2 Hz position control bandwidth.

References

[1] WA Bullough; The third wave of machines; Endeavour; Vol 20; June 1996; ISBN 0160-9327; pp50-55.
[2] N Jakeman, PH Mellor, WA Bullough; Electronic Reconfiguration in Flexible Winding Type Machines; Mechatronics 98 – Proceedings of the 6th UK Mechatronics Forum International Conference, Skovde, Sweden; Elsevier science, Pergamon Publications; ISBN 0-08-043339-1, pp159-165.
[3] K Halbach; Design of permanent magnet multi-pole magnets with orientated rare earth cobalt material; Nuclear instruments and methods vol 169 No 1; 1980; ISSN 0029-554X; pp1-10.
[4] Corvill J; Mechanical engineers data handbook; ISBN 0-7506-1960; pp134.
[5] Howe D, Zhu ZQ, Halbach permanent magnet machines and applications: a review; Electric power applications 148(4); 2001; ISSN 1350-2352; pp299-308.